LOW-NOISE ALN-ON-SI RESONANT INFRARED DETECTORS USING A COMMERCIAL FOUNDRY MEMS FABRICATION PROCESS

Vikrant J. Gokhale[1], Cesar Figueroa[1], Julius Ming Lin Tsai[2], and Mina Rais-Zadeh[1,3]
[1] Department of Electrical Engineering and Computer Science, University of Michigan, Ann Arbor
[2]Invensense Inc., San Jose, CA, USA
[3] Department of Mechanical Engineering, University of Michigan, Ann Arbor, MI, USA

ABSTRACT

This work presents the first measured results for resonant AlN-based infrared (IR) detectors fabricated using a proprietary InvenSense AlN MEMS process. Resonators fabricated in the first fabrication run achieved high electromechanical performance with a *Q* of ~1400 at 115 MHz, insertion loss of 17.9 dB, and a motional impedance of 670 Ω. The detectors are coated with an IR absorber layer (SiN_x), and tested for response to IR radiation using a calibrated, traceable black body source. The estimated responsivity of the device is 210ppb/µW for the longwave-infrared (LWIR) spectrum. The detectors are expected to have low noise, with estimated NEDT and NEP of 51 mK and 52.7 pW/$Hz^{0.5}$, respectively. The resonators are fabricated in a hybrid MEMS/CMOS wafer level packaged die, allowing for CMOS-based routing and readout.

INTRODUCTION

Infrared (IR) detectors have been in use since the 1950s, with the primary uses being surveillance, security and defense, and astronomical imaging. While a number of technically advanced solutions exist for the high sensitivity and resolution requirements of these applications [1], the associated costs make them prohibitive for wide commercial use if high-end performance is to be maintained. The leading candidates for high performance and low cost include uncooled IR detector elements and small- to medium-format focal plane arrays (FPAs) fabricated using MEMS technology [2], [3]. Recent years have shown that piezoelectric electromechanical resonators have the potential to be used as very sensitive, low-noise, small footprint, and low-power uncooled IR detectors [4], [5]. Recent prototypes of single resonators [6], differential pairs [7], and IR sensing arrays [5], [8] have been successfully demonstrated using a variety of materials for the resonator themselves, as well as for the crucial high-efficiency IR absorber layer [9], [10]. The present work successfully transitions designs and processes developed in research labs to a repeatable commercial foundry MEMS/CMOS fabrication process using aluminum nitride (AlN) based resonators.

PROCESS AND DESIGN

Fabrication Process

The devices were fabricated as part of a multi-user wafer using commercial foundry processes at A*STAR IME (MEMS chip with low stress AlN-on-Si) and Global Foundries (CMOS chip) followed by wafer-level bonding at IME. The InvenSense AlN MEMS process begins by preparing an engineered silicon-on-insulator (SOI) wafer with cavities. A bare silicon (Si) wafer is first etched to form cavities on one side, followed by SiO_2 deposition. Next, the wafer with Si cavities is fusion bonded to another Si wafer and thinned down till the required device layer thickness is achieved. In this case, the goal was 5µm for the device layer. An AlN seed layer, bottom metal layer, and structural AlN layer are subsequently deposited. A standoff layer on top of the AlN structural layer is used to define the gap between the MEMS substrate and the CMOS substrate. The AlN structural layer is then patterned. The top metal and Ge layers are deposited and patterned to form top electrodes and AlGe bonding pads corresponding to CMOS top metal pads, respectively. After the contours of the MEMS structure are defined using deep reactive ion etch (DRIE), the MEMS substrate is bonded to a CMOS substrate to form electrical connections with CMOS circuitry. This step also achieves hermetic sealing. At the same time, it also provides extremely low electrical parasitics and a full utilization of the CMOS routing capability without the need for expensive and complicated through-silicon-via (TSV) processing. Finally, the MEMS substrate is thinned down and etched from the back with the port opening to allow direct contact with external environment.

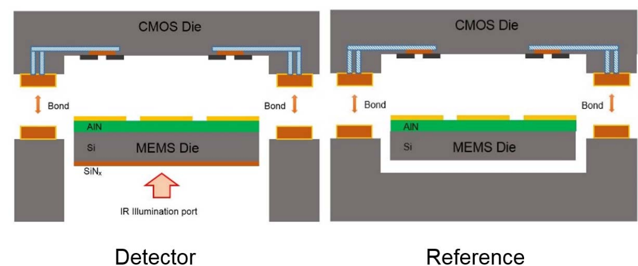

Figure 1: A schematic (not to scale) depicting the AlN-on-Si resonant IR detectors. The sense resonator (left) has an illumination port and is coated with silicon nitride, while the reference resonator (on right) is shielded from IR radiation. The MEMS resonator wafer is bonded to a CMOS readout IC at the wafer level.

Note that in the case of reference resonators used for differential measurements, the port etch (backside DRIE) is not used. The reference is shielded from IR illumination by the MEMS wafer and potentially by another metal shielding layer. Fig. 1 shows schematic cross-sections of both detector and reference resonators, with and without the IR illumination port, respectively. This process is suitable for MEMS devices or arrays of MEMS devices such as IR bolometers as it allows for high 'pixel' packing density without complicated multi-layer routing on the MEMS die. Finally, the bonded wafers are separated by

dicing. Fig. 2 shows a microscope image of such a separated die, as seen from the bottom of the MEMS die. The die is a 4×3 array of AlN-on-Si resonators, with 11 detectors and one reference. Silicon nitride is coated on the device backside at the final step to act as the IR absorber layer (this step is done at the U. of Michigan cleanroom). The reference resonator is shielded from the deposition.

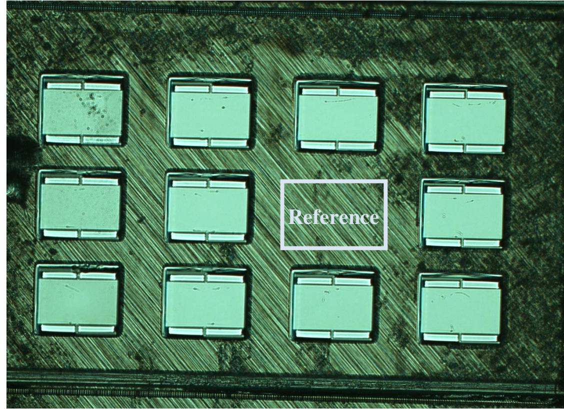

Figure 2: Optical microscope image showing an array of AlN-on-Si resonant IR detectors through their illumination ports (backside of the MEMS die). The reference resonator has no port, thus shielding it from IR radiation.

Design

The devices presented here are in-plane length-extensional mode resonators fabricated using AlN-on-Si as the structural materials. Multiple designs have been implemented in this batch, both as arrays and as single resonators. The resonators intended to work as IR detectors were designed to achieve low noise equivalent temperature difference (NETD) values (< 50 mK). One of the key factors in getting low NETD is to improve the thermal isolation of the resonators, specifically by decreasing the effective thermal conductance (G_{th}) of the tethers [4], [8]. One useful technique is to use crableg tethers instead of conventional straight tethers [10]. This increases the effective tether length (and thus decreases tether conductance) without decreasing the ratio of active absorbing area to the total etch cavity area which is the optical fill factor of the resonator pixel. As seen in Fig. 3, it is possible to get an effective tether length of 120 µm without sacrificing the fill factor. Simulations were used to determine the correct dimensions for the tethers to increase thermal isolation while at the same time not compromising the electromechanical performance of the resonator.

EXPERIMENTAL RESULTS

RF Performance of Resonators

The resonator demonstrates a high Q of 1380 at 115 MHz and a reasonably low insertion loss at -10 dBm of RF input (Fig. 4). Using an equivalent electrical model, we can calculate the motional impedance to be 670 Ω.

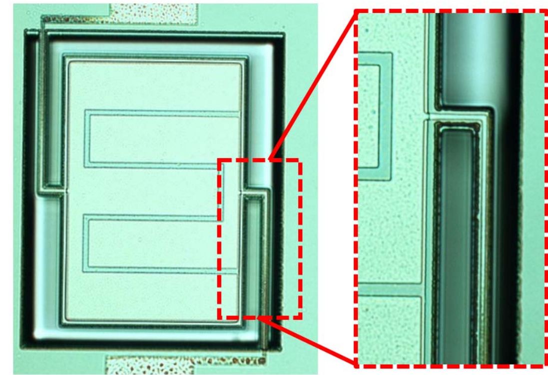

Figure 3: Optical microscope image of a sense resonator. This resonator is 190 µm × 128 µm in size. Magnified portion of the image highlights the use of a crableg tether that increases the thermal isolation of the device (desirable for high sensitivity and low noise), while retaining a compact total pixel size. The effective length of each tether is 120 µm. This image is taken from a deliberately de-bonded die to expose the resonator.

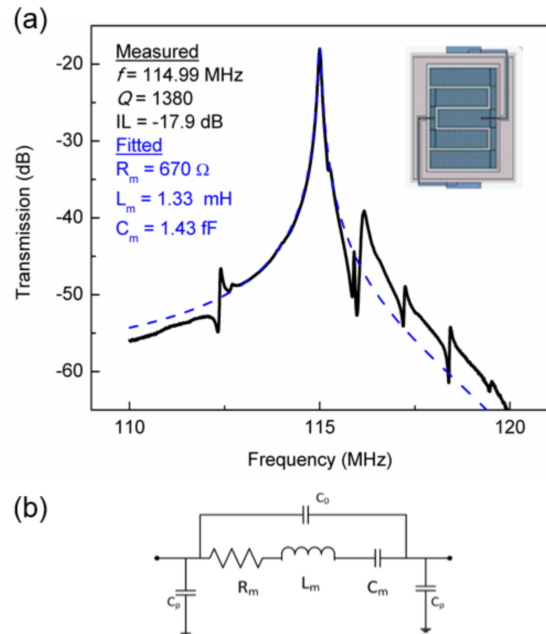

Figure 4: (a) Measured response of the AlN-on-Si resonator fabricated using a commercial foundry MEMS process, when actuated with -10 dBm of RF power. (b) BVD model of the two-port resonator.

Other devices from the same batch that had simple, straight conventional tethers (not crableg) were also tested. The RF performance of those devices is comparable to the crableg device measured here, with f×Q values in the same range. As expected the devices with the simple tethers show markedly worse IR performance.

Infrared Response of the Prototype Resonators

The AlN-on-Si resonators are characterized for their IR performance in both near IR (NIR) and LWIR spectra. For the LWIR spectrum, we use a large area black body radiation source (Electro-Optical Industries' LES-100-4)

with an emissivity of (0.97 ± 0.02), a temperature stability of ± 2 mK, and a planar emitting area of 102 mm × 102 mm. The source is freshly calibrated, and is traceable to NIST primary standards [11]. The high emissivity and temperature stability enable us to calculate the exact power distribution as a function of temperature and area of the source, according to the Stefan-Boltzmann Law. Given far-field radiation conditions and the known size of the resonator surface, we can calculate the power incident on the device. The resonant frequency of the device changes upon illumination with IR radiation, due to the absorption of radiation (in the IR absorber layer) and the subsequent conversion of that absorbed power into a temperature change in the resonator. Fig. 5 shows the IR measurement setup.

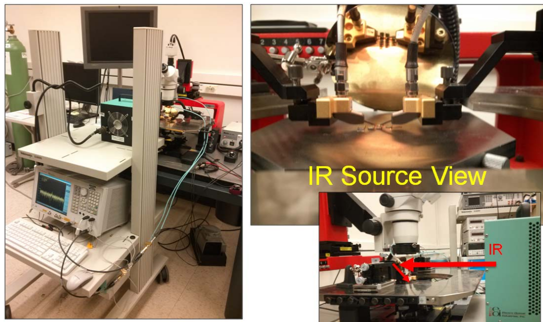

Figure 5: A photograph of the measurement setup. The device under test is mounted on a probe station, and its RF performance is measured using an Agilent VNA. For IR measurements, the device is illuminated using a wide-area black body source and a highly reflective gold mirror. All measurements are acquired remotely using a PC running custom-made LabVIEW code.

Fig. 6 shows a representative frequency response of a resonator to IR radiation when the source is at 80 °C (353 K). Based on the known temperature coefficient of frequency (TCF) and area of the devices, we can estimate the absorbed LWIR power to be ~3.1 µW (See Table 1).

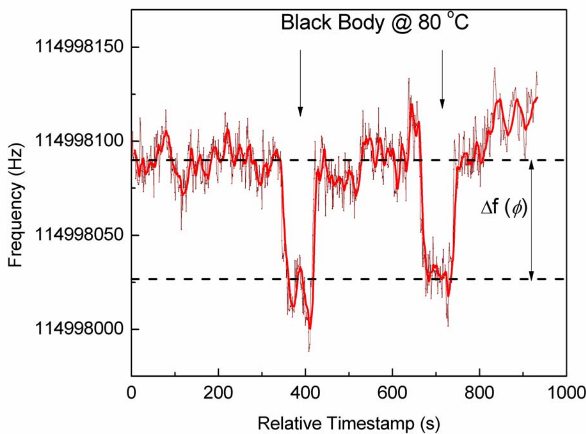

Figure 6: The frequency response of the device when irradiated by blackbody radiation from the calibrated source at 80 °C. The resonator absorbs ~ 3.1 µW of IR power in the LWIR spectra, leading to a perceptible frequency shift. This particular experiment was carried out in ambient air, with no temperature control.

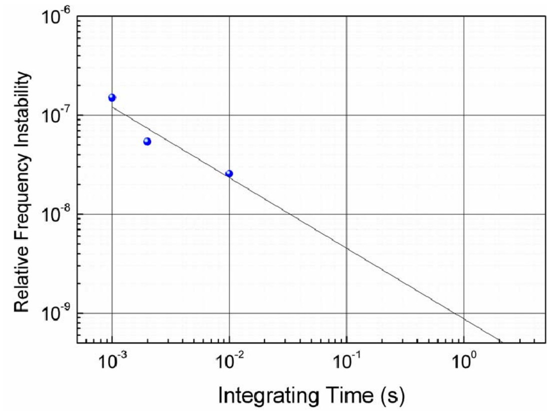

Figure 7: The relative frequency instability of the device as a function of integrating time. Measurements are acquired at ambient conditions, with no temperature or pressure control. For integrating time> 10 ms, the values are extrapolated. As expected, the device is more stable with larger integration times.

In order to characterize the differential performance of the resonators, we compare the IR response of two nearly identical detectors (with silicon nitride absorber) and one reference (without silicon nitride absorber). As expected, the reference is nearly invariant to stimulus. Using a near-IR radiation source (Ocean Optics HL2000) and fiber-optic probes to couple light onto the specific resonators in questions we can compare the relative response (Fig. 8). Differential measurements can enable highly sensitive systems with common mode rejection of common mode effects. Details of the procedure and differential measurements are provided in our previous work [8]. For the NIR spectrum, the absorbed power is ~2.47 µW.

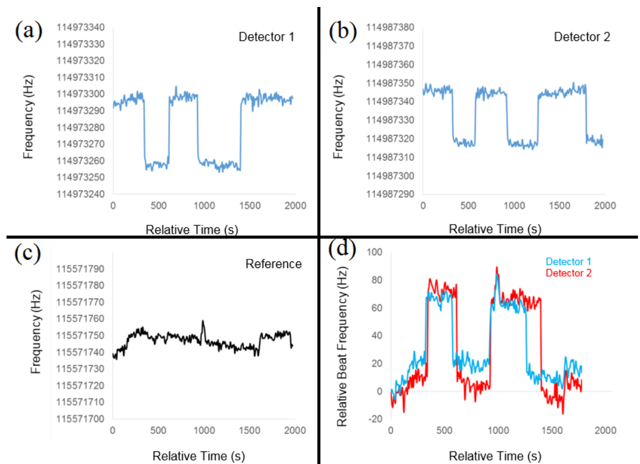

Figure 8: (a)-(c) The frequency response of two detectors and a reference when irradiated by NIR radiation. Note that the Y-axes have the same scales for these three graphs. The absorbed power is estimated to be on the order of ~ 2.47 µW of IR power leading to a perceptible frequency shifts in the detector but near-zero shift in the reference. (d) Using the relative beat frequency between detectors and reference we can achieve differential IR sensing.

Expected Infrared Metrics

Based on the design parameters and material properties of the resonators (Table 1), the AlN-on-Si resonant detectors are expected to have low-noise performance, with calculated NETD and NEP values of 51 mK and 52.7 pW/$Hz^{0.5}$, respectively [12]. Low NEDT is especially desirable, with commercial uncooled bolometer FPAs exhibiting NETD values on the order of 30 mK [13].

To an extent, the low NETD for these particular devices is due to the large surface area of the devices. For resonator pixels intended to be part of an IR imager, the area of the individual device must be reduced significantly. In order to keep NETD values at the same level, it is necessary to improve the thermal isolation of the devices (reduce G_{th}). For the current batch, the designs were primarily constrained by the process limitations of a multi-project fabrication process and the relatively large thickness of the Si device layer. With thinner and narrower tethers optimized for high thermal isolation, it is possible to get up to two orders of magnitude improvement in G_{th}, responsivity, and noise. Designs fabricated in the recent past [6], [10] using AlN-based resonant IR detectors have experimentally demonstrated thermal conductance as low as 10^{-5} W/K with the potential to go even lower.

Table 1. Design & Expected Performance Parameters for the Presented AlN-on-Si Resonant IR Detector.

Design Parameter	Value	Performance Metric	Value
Resonator Length	190 µm	Frequency	115 MHz
Resonator Width	128 µm	*Q*	1380
Tether Length	120 µm (Crableg)	Absorber	Silicon nitride
TCF	-30 ppm/K	Responsivity (LWIR)	210 ppb/µW
G_{th} (2 crableg tethers)	1.42 ×10^{-4} W/K	NETD (calculated)	51 mK
		NEP (calculated)	52.7 pW/$Hz^{0.5}$

CONCLUSION

This work lays the groundwork for high-performance uncooled, resonant IR detectors and detector arrays based on a commercially available and commercially viable technology. The success of this design and fabrication cycle is promising for better, more optimized processes and designs. The integration of resonant IR detectors with electronics and other MEMS based components on the same die would add significant functionality to commercial sensing and position control solutions. Similar resonators and arrays can also be used for a variety of other applications such as timing, mass sensing, flow-rate sensing, and biological/chemical sensing with only slight changes in the current designs.

ACKNOWLEDGEMENTS

The authors would like to thank Mr. Adam Peczalski for assistance with the silicon nitride deposition. The work is supported by the MAST CTA under contract W911NF.

REFERENCES

[1] A. Rogalski, "Infrared detectors: status and trends," *Progress in Quantum Electronics*, vol. 27, pp. 59-210, 2003.

[2] M. Kimata, "Trends in small-format infrared array sensors," *IEEE SENSORS*, pp. 1-4, 2013.

[3] A. Rogalski, "Recent progress in infrared detector technologies," *Infrared Physics & Technology*, vol. 54, pp. 136-154, 2011.

[4] J. R. Vig, R. L. Filler, and Y. Kim, "Uncooled IR imaging array based on quartz microresonators," *IEEE/ASME Jounal of Microelectromechanical Systems (JMEMS)*, vol. 5, pp. 131-137, 1996.

[5] P. Kao and S. Tadigadapa, "Micromachined quartz resonator based infrared detector array," *Sensors and Actuators A: Physical*, vol. 149, pp. 189-192, 2009.

[6] Y. Hui, Z. Qian, G. Hummel, and M. Rinaldi, "Pico-watts range uncooled infrared detector based on a freestanding piezoelectric resonant microplate with nanoscale metal anchors," *Solid-State Sensors, Actuators and Microsystems Workshop*, Hilton Head Island, South Carolina, 2014.

[7] V. J. Gokhale, Y. Sui, and M. Rais-Zadeh, "Novel uncooled detector based on gallium nitride micromechanical resonators," *Proceedings of SPIE: Infrared Technology and Applications*, vol. 8353, p. 835319, 2012.

[8] V. J. Gokhale and M. Rais-Zadeh, "Uncooled infrared detectors using gallium nitride on silicon micromechanical resonators," *IEEE/ASME Journal of Microelectromechanical Systems (JMEMS)*, vol. 23, pp. 803 - 810, 2014.

[9] V. J. Gokhale, O. A. Shenderova, G. E. McGuire, and M. Rais-Zadeh, "Infrared absorption properties of carbon nanotube/nanodiamond based thin film coatings," *IEEE/ASME Journal of Microelectromechanical Systems (JMEMS)*, vol. 23, pp. 191-197, 2014.

[10] V. J. Gokhale, P. D. Myers, and M. Rais-Zadeh, "Subwavelength plasmonic absorbers for spectrally selective resonant infrared detectors," *IEEE Sensors*, Valencia, Spain, 2014.

[11] E.-O. Industries. (2014). Available: http://www.electro-optical.com/pdf/LES100-RevB.pdf

[12] P. W. Kruse, Uncooled Thermal Imaging: Arrays, Systems, and Applications. Bellingham, Washington, USA: SPIE Press, 2001.

[13] F. Niklaus, C. Vieider, and H. Jakobsen, "MEMS-based uncooled infrared bolometer arrays: a review," *Proc. SPIE*, vol. 6836, pp. 68360D-68360D, 2007.

CONTACT

*M. Rais-Zadeh, email: minar@umich.edu